Biometals (2013) 26:805–812
DOI 10.1007/s10534-013-9660-0

Catalytic and regulatory roles of species involved in metal–nucleotide equilibriums in human pyridoxal kinase

Freddy Navarro · César A. Ramírez-Sarmiento · Victoria Guixé

Received: 28 January 2013 / Accepted: 10 July 2013 / Published online: 17 July 2013

Abstract Pyridoxal 5′-phosphate is the active form of vitamin B_6 and its deficiency is directly related with several human disorders, which make human pyridoxal kinase (hPLK) an important pharmacologic target. In spite of this, a carefully kinetic characterization of hPLK including the main species that regulates the enzymatic activity is at date missing. Here we analyse the catalytic and regulatory mechanisms of hPLK as a function of a precise determination of the species involved in metal–nucleotide equilibriums and describe new regulatory mechanisms for this enzyme. hPLK activity is supported by several metals, being Zn^{2+} the most effective, although the magnitude of the effect observed is highly dependent on the relative concentrations of metal and nucleotide used. The true substrate for the reaction catalyzed by hPLK is the metal nucleotide complex, while ATP^{4-} and $HATP^{3-}$ did not affect the activity. The enzyme presents substrate inhibition by both pyridoxal (PL) and $ZnATP^{2-}$, although the latter behaves as a weakly inhibitor. Our study also established, for the first time, a dual role for free Zn^{2+}; as an activator at low concentrations (19 μM optimal concentration) and as a potent inhibitor with a IC_{50} of 37 μM. These results highlighted the importance of an accurate estimation of the actual concentration of the species involved in metal–nucleotide equilibriums in order to obtain reliable values for the kinetic parameters, and for determine the true regulators of the PLK activity. They also help to explain the dissimilar kinetic parameters reported in the literature for this enzyme.

Keywords Human pyridoxal kinase · Divalent metal cation · Enzyme inhibition · Metal–nucleotide complex · Zinc

Introduction

Pyridoxal 5′-phosphate (PLP) is the active form of vitamin B_6, being one of the most important and versatile cofactors in nature. This intracellular active form of vitamin B_6 is the cofactor for many enzymes such as aminotransferases and decarboxylases. Almost all the PLP dependent enzymes known to date are involved in biochemical pathways related with amine compounds, mainly amino acids (Percudani and Peracchi 2003). In many bacteria and plants, PLP is synthesized by a de novo pathway, but mammals depend on the exogenous source of vitamin B_6, i.e. pyridoxine, pyridoxal and pyridoxamine. Usually these cells have a salvage pathway for reutilizing the pyridoxal (PL) liberated during protein turnover, where

Electronic supplementary material The online version of this article (doi:10.1007/s10534-013-9660-0) contains supplementary material, which is available to authorized users.

F. Navarro · C. A. Ramírez-Sarmiento · V. Guixé (✉)
Laboratorio de Bioquímica y Biología Molecular, Departamento de Biología, Facultad de Ciencias, Universidad de Chile, Casilla 653, Santiago, Chile
e-mail: vguixe@uchile.cl

the enzyme pyridoxal kinase (PLK) is a fundamental step (McCormick et al. 1961; di Salvo et al. 2011). PLP deficiency is directly related with human disorders (Cao et al. 2006), and for this reason human PLK (hPLK) is an important pharmacologic target for the regulation of PLP amounts. In this sense understanding the catalytic and regulation features of this enzyme, is crucial for the development of pharmacologic drugs.

The crystal structure of PLK from different sources shows a dimeric structure with one active site per each monomer (Gandhi et al. 2009; Newman et al. 2006; Cao et al. 2006; Safo et al. 2006; Li et al. 2002). Recently hPLK structure in complex with neurotoxins (Gandhi et al. 2012) and *T. brucei* PLK structure in complex with ATP (Jones et al. 2012) have been reported. Structurally, PLK belongs to the ribokinase superfamily whose members shared a Rossman-like fold, with a central β-sheet composed of mainly parallel strands and eight α-helices, five in one side and three on the other, which is known as the large domain (Zhang et al. 2004). Additionally, some of the members of the superfamily present a smaller domain. However, PLK lacks this structure but the sheep brain enzyme presents a key 12-residue loop that lies over the active site when substrates are bound. The corresponding segment in hPLK is not a loop, but a β-strand/loop/β-strand flap. It has been suggested that the length and sequence of this peptide might serve as an evolutive marker of the PLK family (Li et al. 2002).

Functionally, ribokinase superfamily members catalyze the phosphorylation of an alcohol group on small aromatic molecules or carbohydrates. In particular, PLK catalyzes the phosphorylation of pyridoxine, pyridoxamine and pyridoxal to form pyridoxine 5′-phosphate, pyridoxamine 5′-phosphate and PLP, respectively. Pyridoxine 5′-phosphate and pyridoxamine 5′-phosphate are subsequently converted to PLP by pyridoxine 5′-phosphate oxidase.

With respect to the phosphoryl donor, PLK can use ATP complexed with a divalent metal cation (M^{2+}), like Zn^{2+} or Mg^{2+}. Although studies with the human, sheep, and pig brain PLK have shown that $ZnATP^{2-}$ is the preferred substrate, di Salvo et al. (2004) concluded that under physiological conditions $MgATP^{2-}$ would be the favoured one for the *E. coli* kinases. In contrast the enzyme from *T. brucei* uses preferentially Mg^{2+} or Mn^{2+} being Zn^{2+} almost ineffective (Jones et al. 2012). However, for enzymes that use a metal–nucleotide as a substrate, the different equilibriums between the several possible ionic species present at the pH employed has to be considered (Sigel 2004). This is especially important for hPLK since its activity is usually measured at pH 6.5 where the prevalence of others species besides $M^{2+}ATP^{2-}$, cannot be ignored. One of these species is $HATP^{3-}$, which can act as an inhibitor or by limiting the amount of free ATP^{4-} present for substrate formation (Storer and Cornish-Bowden 1976; Tribolet and Sigel 1988). Early reports on PLK characterization mention the fact that several metal ions can activate PLK from rat liver, highlighting that Zn^{2+} was markedly superior to Mg^{2+} for the purified enzyme over a large range of concentrations of added cation (McCormick et al. 1961). Nevertheless, in these experiments the lowest concentration of metal used is far below the ATP concentration (0.5 mM), and then the activation observed may be due to the increase in the true substrate concentration (metal–nucleotide complex). Also, the preliminary kinetic characterization of hPLK available to date does not consider all the species present in solution, such as ATP^{4-}, $HATP^{3-}$ and the free metal concentration, which varies its concentration depending on the pH employed. Particularly, the effect of this later species on the enzyme activity has not been described. Specifically, emphasis has been directed toward sorting out which ligand is the required substrate and which act as activators or inhibitors, since a carefully kinetic characterization of human PLK including the main species that regulates the enzymatic activity is at date missing. In this work we analyse the catalytic and regulatory mechanisms of hPLK as a function of a precise determination of the species involved in metal–nucleotide equilibriums and describe new regulatory mechanisms for this enzyme.

Materials and methods

Purification of hPLK

E. coli strain BL21(DE3) was transformed with the p24a-LIC-hPLK vector, coding for hPLK and six histidines in the N-terminal. The transformed strain was denominated BL21-p24a-hPLK. Growing of the BL21-p24a-hPLK strain and induction and purification of hPLK were performed essentially as described by the Ismail group (Ismail et al. 2005). Briefly, the supernatant was passed through a DE52 column equilibrated with 10 mM Tris HCl pH 7.5, 0.5 M NaCl, 5 % glycerol,

10 mM β-mercaptoethanol, and 5 mM imidazole and then loaded into a Ni–NTA column equilibrated with the same buffer. The column was washed with 10 mM Tris–HCl pH 7.5, 0.5 M NaCl, 5 % glycerol, 10 mM β-mercaptoethanol, and 30 mM imidazole and the protein eluted using 10 mM Tris–HCl pH 7.5, 0.5 M NaCl, 5 % glycerol, 10 mM β-mercaptoethanol and 250 mM imidazole. Fractions with hPLK activity were pooled and dialyzed against 50 mM Tris–HCl pH 7.5, 5 % glycerol and 10 mM β-mercaptoethanol. Protein was concentrated and 5 mM $MgCl_2$ and 10 mM DTT were added. Protein was storage at a concentration of 2 mg mL^{-1} in 50 % glycerol at −20 °C.

Activity measurements and kinetics studies

Enzyme activity was measured by following the increase in absorbance at 388 nm, using a molar extinction coefficient determined by us at pH 6.5 and 37 °C with 20 mM PIPES, which corresponds to 2687.5 cm^{-1} M^{-1}. One enzymatic unity (U) is defined as the amount of nanomoles of PLP formed per minute. The assays were performed at 37 °C in a Hewlett Packard 8453 spectrophotometer.

Kinetic constants were calculated assuming a steady state condition. To determine the K_m value for PL, the concentration of substrate was gradually varied, while leaving constant the concentrations of the other species. In order to obtain the K_m for $ZnATP^{2-}$, the concentration of PL and Zn^{2+} remains constant whereas the $ZnATP^{2-}$ concentration was progressively varied. All tests were performed using 20 mM PIPES at pH 6.5 and 5 μg of protein (0.18 μM). To evaluate the effect of $HATP^{3-}$ and ATP^{4-} on the PLK activity, the concentration of ATP (disodium salt, microbial source, Sigma) and $ZnCl_2$ was varied gradually, always with an excess of ATP, in a 5:1 ratio, at pH 6.5 with 20 mM PIPES, and at pH 8.0 with 20 mM HEPES. For example, at pH 6.5, the lowest $ZnCl_2$ concentration employed was 0.02 mM to achieve a $ZnATP^{2-}$ concentration of 0.0105 mM, while the highest concentration of $ZnCl_2$ assayed was 5 mM mM to obtain a $ZnATP^{2-}$ concentration of 4.867 mM.

The experimental curves were fit to Michaelis–Menten equation and non-Michaelis–Menten kinetics with substrate inhibition. Linear and nonlinear regressions were performed using the program Sigma Plot 10.0 (Systat Software, Inc.).

For tested hPLK metal specificity, eight divalent metals were employed (Ca^{2+}, Mg^{2+}, Mn^{2+}, Co^{2+}, Ni^{2+}, Cu^{2+}, Zn^{2+}, and Cd^{2+}), at a final total concentration of 0.1 mM, 0.5 mM and 1.5 mM The reaction mix contained 3.5 mM PL, 0.5 mM ATP, 20 mM PIPES at pH 6.5, and 5 μg of protein (0.18 μM).

Estimation of the concentration of the species involved in the metal–nucleotide equilibrium

The actual concentration of the species involved in the metal–nucleotide equilibrium was calculated using the respective dissociation constant of each particular equilibrium at 37 °C (Abercrombie and Martin 1980) and considering the pH of the solution (Cornish-Bowden 1995). The constants used were:

Reaction	Ka (M^{-1})
$Zn^{2+} + HATP^{3-} \rightleftarrows ZnHATP^{-}$	3.95×10^2
$Zn^{2+} + ATP^{4-} \rightleftarrows ZnATP^{2-}$	5.47×10^4
$H^{+} + HATP^{3-} \rightleftarrows H_2ATP^{2-}$	8.12×10^3
$H^{+} + ATP^{4-} \rightleftarrows HATP^{3-}$	1.03×10^7

The calculations were performed according to the suggestions of Storer and Cornish-Bowden (1976) and were performed in Scilab 4.1.2 software.

Effect of pH on hPLK activity

Estimation of the optimum pH was achieved by varying the pH between 4.0 and 10.0 using the following buffers: acetate (pH 4.0 - 5.5), MES (pH 6.1), HEPES (pH 6.8 to 8.2) and carbonate (pH 8.9 to 10.0). All buffers were used at a final concentration of 20 mM in the presence of 2.5 mM PL, 2.5 mM ATP, 0.5 mM total Zn^{2+} and 5 μg of total protein. We determine the effect of the buffer on the enzyme activity by using more than one buffer for the same pH. For the pH curve (Fig. 3) we show those buffers for which the greatest initial velocities were obtained.

Results and discussion

Effects of divalent cations on the activity of hPLK and determination of kinetic parameters

Mammalian and prokaryotic PLK requires divalent cations for its activity. The requirement of divalent cations for catalysis is mandatory for hPLK, since in

the absence of any divalent ion, the enzyme exhibits no catalytic activity. Figure 1 shows the effect of several divalent cations tested to support hPLK activity. The data indicate that several metals are able to support the activity, being Zn^{2+} Mg^{2+}, Mn^{2+} and Co^{2+} the most effective. However, the magnitude of the effect observed is highly dependent on the relative concentrations of metal and nucleotide used. Cd^{2+}, Cu^{2+} and Ca^{2+} presents only minor differences in the enzymatic activity in the three conditions tested, that is when the metal concentration is below the ATP concentration, when metal and nucleotide are at equimolar concentrations or when the metal concentration is 3 times higher with respect to the nucleotide concentration. In contrast, the hPLK activity increases concomitantly with increasing concentrations of Mg^{2+}, while Mn^{2+} and Co^{2+} shows inhibition of the enzyme activity when the metal exceeds the nucleotide concentration. Zn^{2+} constitutes a special case since the highest activity is observed with this metal and also the activity diminishes dramatically as the concentration of Zn^{2+} increases. The fact that Zn^{2+} was the most effective divalent cation for catalysis has been demonstrated for PLK from several sources (McCormick et al. 1961; Lee et al. 2000; Lum et al. 2002). Nonetheless, in these cases the concentration of divalent metal cation is far below the ATP concentration (0.1 mM Zn; 0.5 mM ATP), which raise several caveats regarding the interpretation of the results. For example, in both the work of Lee et al. (2000) and in Lum et al. (2002) the relative activity for Mg^{2+} was underestimated mainly because the metal concentration used was not enough to complex the nucleotide. Here, we show that the relative activity of hPLK rises from 10 to 45 % when Mg^{2+} concentration increases from 0.5 to 1.5 mM at a fixed ATP concentration of 0.5 mM (Fig. 1).

In order to determine the kinetic parameters for substrates in the presence of Zn^{2+}, the hPLK activity was assayed as a function of PL and $ZnATP^{2-}$ concentration. When PL was varied, enzyme inhibition was observed at concentrations above 4–5 mM, reaching a plateau at a value of 25 % of the maximal activity (Fig. 2a). On the other hand, saturation curve for $ZnATP^{2-}$, shows a slightly inhibition at concentrations above 0.6 mM (Fig. 2b). Although PL inhibition was described previously in two studies (McCormick et al. 1961; Neary and Diven 1970), $ZnATP^{2-}$ inhibition has not been reported. There is only one mention to

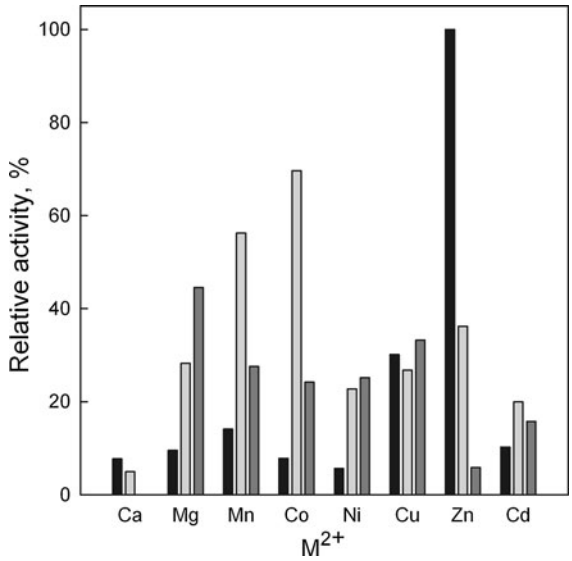

Fig. 1 Divalent metal cation dependence of hPLK. Enzyme assays were performed with different metal concentrations: 0,1 mM total M^{2+} (*black filled bar*), 0,5 mM total M^{2+} (*light grey filled bar*), and 1,5 mM total M^{2+} (*dark grey filled bar*).The assay mixture contained 20 mM PIPES at pH 6.5, 3.5 mM PL, 0.5 mM ATP and 5 μg of PLK. Assays were performed in duplicate

inhibition by $ZnATP^{2-}$ in the *E. coli* enzyme in the paper of di Salvo et al. (2004) who report inhibition at concentrations above 50–100 μM. However, in this report the authors did not mentioned the metal concentration used and then it may be possible that the inhibition observed was due to the free metal concentration present in the solution. Table 1 summarizes the kinetic parameters for hPLK. The difference observed in the k_{cat} value can be due to the dissimilar free Zn^{2+} concentration used in both experiments.

Nonetheless, the usual initial velocity studies where the concentration of one ligand is varied at several fixed concentrations of the other are complicated because M^{2+}, ATP^{4-} and M-ATP^{2-} cannot be varied independently of each other due to the equilibrium between them (Table S1). In these analyses, the concentrations of free and complexed species must be calculated whenever the concentration of any species is changed. Moreover, considering the pH employed for measuring PLK activity, varying the concentration of $ZnATP^{2-}$ at a constant free Zn^{2+} concentration implies necessarily variation in the $HATP^{3-}$ and ATP^{4-} concentrations. For example, when PL concentration was varied, the concentration of $ZnATP^{2-}$, ATP^{4-}, $HATP^{3-}$ and free Zn^{2+} can held constant.

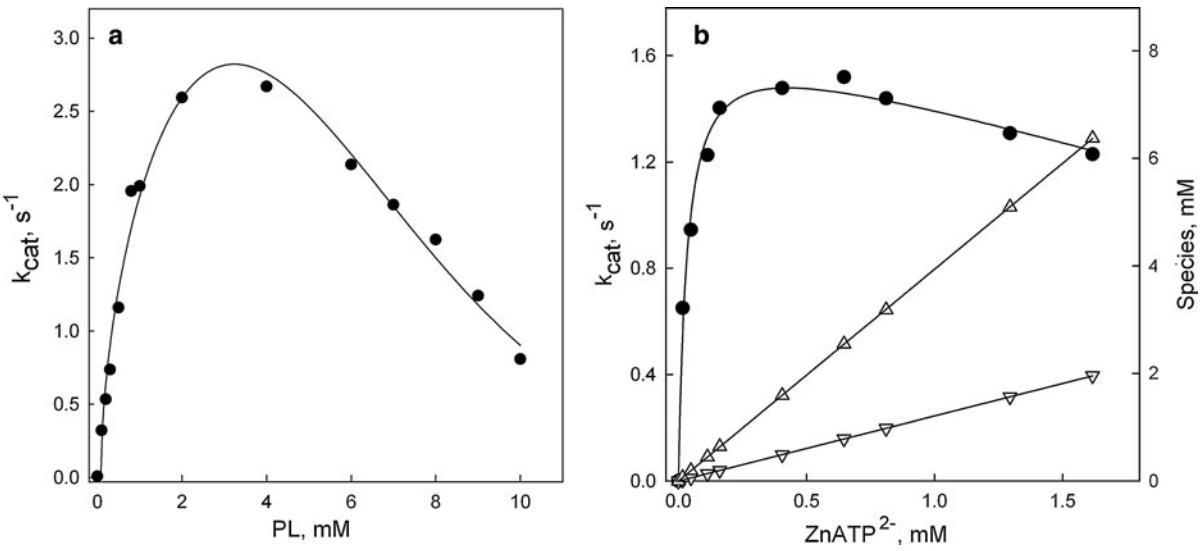

Fig. 2 Saturation curves for PL and $ZnATP^{2-}$. **a** hPLK activity as a function of PL. Concentration of other species was constant: 473 μM ATP^{4-}; 1.54 mM $HATP^{3-}$; 19 μM free Zn^{2+}; 470 μM $ZnATP^{2-}$. **b** hPLK activity as a function of $ZnATP^{2-}$. The variation in the concentration of $HATP^{3-}$ (*upright unfilled triangle*) and ATP^{4-} (*inverted unfilled triangle*) is also shown. PL and free Zn^{2+} concentrations are 2.5 mM and 15 μM, respectively

Table 1 Kinetic parameters of human PLK

	$ZnATP^{2-}$	PL
K_m (μM)	20[a]	490[a]
V_{max} (U/mg)	2788	4789
k_{cat} (s^{-1})	1.9	3.2

[a] Km values were calculated from concentration range where inhibition of enzyme activity was not observed

However, when $ZnATP^{2-}$ is varied, the concentration of $HATP^{3-}$ and ATP^{4-} also does and then the effect of these species on the enzyme activity must be determined. For this purpose we take advantage of the concentration dependence of these species with the pH, so the assays were made at pH 6.5 and 8.0. In first place, we analyse the dependence of the PLK activity with the pH (Fig. 3) where a value of 6.4 was determined as the pH optimum, in accordance with data reported by others authors (Neary and Diven 1970; McCormick et al. 1961). At pH 6.5 the species that increases its concentration more importantly is $HATP^{3-}$ (to 15.3 mM) whilst the ATP^{4-} concentration reaches a value of 4.7 mM. Contrary, at pH 8.0 the ATP^{4-} concentration is 18.1 mM, while the $HATP^{3-}$ concentration is 1.9 mM (Fig. 4a, b). The variation in the maximum activity at both pHs is entirely due to the action of pH, since the maximum activity is reached at the same $ZnATP^{2-}$ concentration, being the value at pH 8.0, 42 % of that determined at pH 6.5, in perfect agreement with the ratio of activities at these two pHs values determined from the pH curve. At both pHs inhibition by $ZnATP^{2-}$ was observed with essentially the same profile even though ATP^{4-} and $HATP^{3-}$ concentrations vary considerably in each condition (Table S2). This ruled out any inhibitory effect that these species could have on the PLK activity and established unambiguously the $ZnATP^{2-}$ as the inhibitory species.

Comparison of kinetic constants determined in this work with those reported previously in the literature is complicated because of the different experimental conditions employed (presence of Na, pH, etc.). For example, Gandhi et al. (2009) reports K_m values of 24 μM for PL and 190 μM for MgATP. However, these authors include sodium in the reaction mixture, the measurements were performed at pH 7.2 and did not mentioned the metal concentration used. On the other hand, di Salvo et al. (2004) reported a K_m value of 350 μM for PL in human PLK using $ZnATP_2$- as co-substrate whereas the K_m for $ZnATP^{2-}$ was not determined because of inhibition of this substrate above 50 μM. These experiments were performed at pH 6.1, in the presence of Na^+ and the concentration of the co-substrate was achieved by held $ZnCl_2$

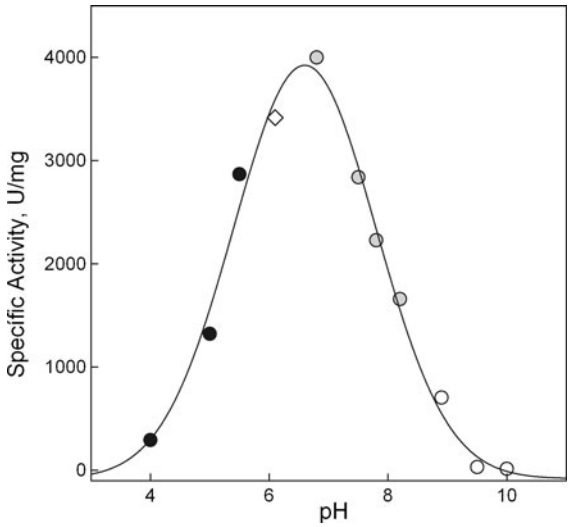

Fig. 3 pH dependence of PLK activity. Enzyme activity at different pH was determined using the following buffers: acetate (*black filled circle*); MES (*diamond*); HEPES (*grey filled circle*) and carbonate (*unfilled circle*)

concentration constant at 50 μM with ATP at 200 mM.

Regulation of PLK activity by free Zn^{2+} concentrations

The other relevant species present in metal–nucleotide equilibriums is the free metal. In order to determine the role of this species on the PLK activity, we performed assays where the $ZnATP^{2-}$ concentration was held constant at 0.5 mM whereas the concentration of free Zn^{2+} increase and both $HATP^{3-}$ and ATP^{4-} concentration decrease. The results show that at low free Zn^{2+} concentration PLK activity increases reaching a maximum at 19 μM, whereas above this value a significant inhibition was observed. The effect of $HATP^{3-}$ and ATP^{4-} can be ruled out because inhibition of enzyme activity is observed even when the concentration of these species is zero (Fig. 5a). From these data an IC_{50} of 37 μM for free Zn^{2+} was determined at pH 6.5 (Fig. 5b). These results established for the first time a dual role of free Zn; as an activator at low concentrations and as a potent inhibitor in the micromolar range. Interestingly, free Mg^{2+} do not inhibit hPLK activity (Fig 1).

In the literature there are various data regarding the kinetic properties of hPLK (Lee et al. 2000; di Salvo et al. 2004; Gandhi et al. 2009). In most cases the

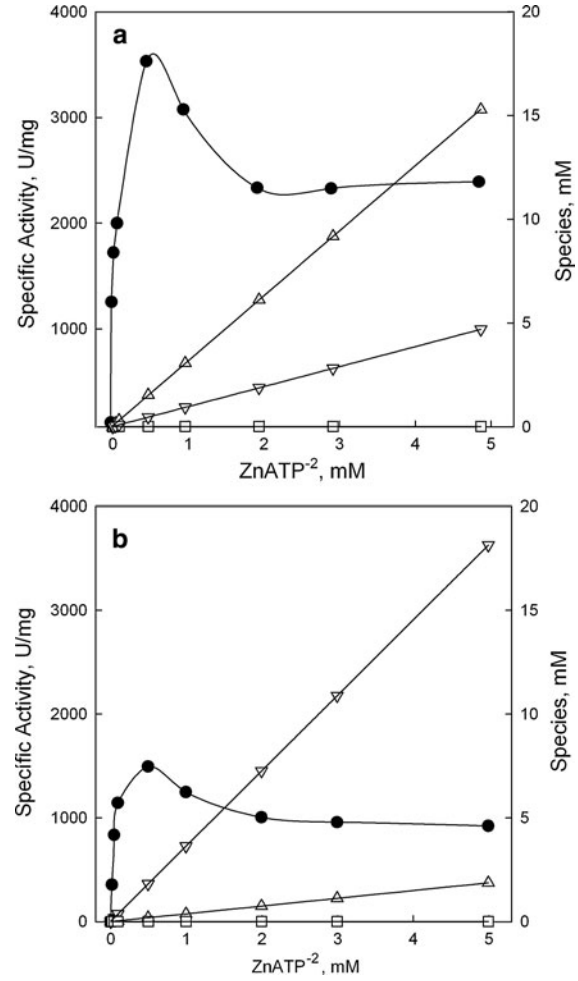

Fig. 4 Variation of species involved in metal–nucleotide equilibriums as a function of pH and $ZnATP^{2-}$. The relative concentration of ATP and $ZnCl_2$ was varied in a 5:1 relationship and the PL concentration was 1.5 mM. The lowest $ZnCl_2$ and ATP concentrations used were 0.02 mM and 0.1 mM while the higher concentrations were 5 mM and 25 mM respectively. **a** Assays performed at pH 6.5; **b** assays performed at pH 8.0. hPLK specific activity (*black filled circle*); free Zn^{2+} (*unfilled square*); ATP^{4-} (*inverted unfilled triangle*) and $HATP^{3-}$ (*upright unfilled triangle*)

kinetic constants are obtained using Mg^{2+} or Zn^{2+}, and the K_m are calculated assuming ATP as the true substrate, even though it has been proposed that the true substrate for most of the kinases studied is the M^{2+}-ATP^{2-} complex (Amsler and Sigel 1976). The reported kinetic parameters for hPLK and for PLK from other species vary widely. This fact is mainly due to the uncontrolled experimental conditions regarding the species involved in metal–nucleotide equilibriums.

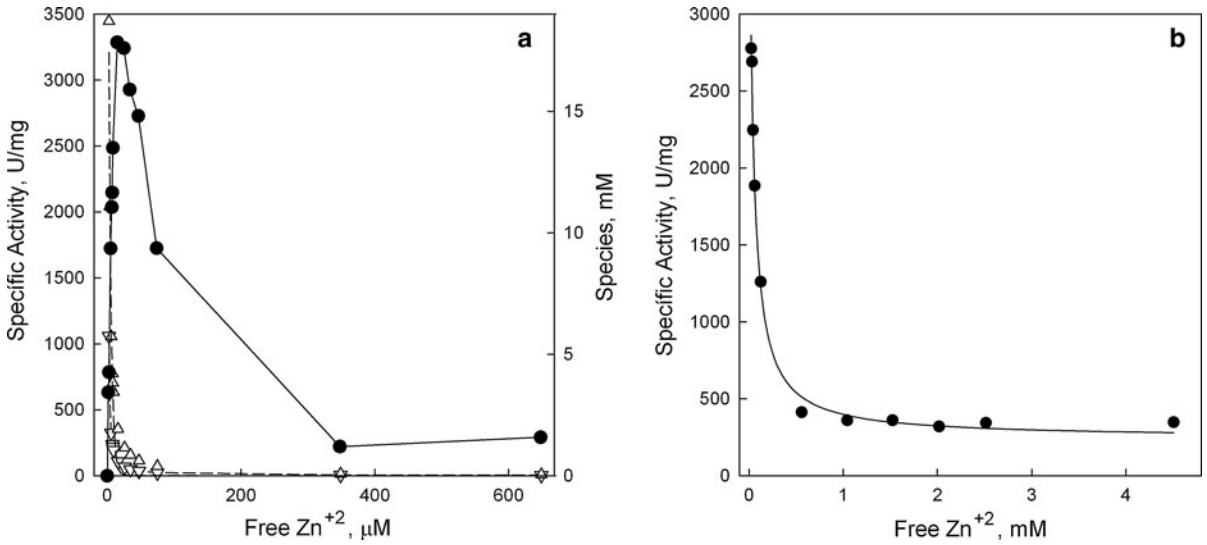

Fig. 5 Effect of free Zn^{2+} concentration on the hPLK activity. **a** PLK activity as a function of free Zn^{2+} concentration at pH 6.5 (*black filled circle*). The variation in the concentration of ATP^{4-} (*inverted unfilled triangle*) and $HATP^{3-}$ (*upright unfilled triangle*) is also shown. **b** The complete range of inhibitory free Zn^{2+} concentrations is depicted. $ZnATP^{2-}$ and PL concentrations were 480 μM and 2.5 mM respectively

For example, in the work of di Salvo et al. (2004) with hPLK, the total concentrations of Zn^{2+} and ATP^{4-} at pH 7.3 were 50 and 200 μM respectively, so the free Zn^{2+} concentration is 8 μM, far below the optimal value of 19 μM determined in this work. On the other hand, the paper of Kästner et al. (2007) reported a total concentration of Zn^{2+} and ATP^{4-} at pH 6.2 of 100 μM and 1 mM respectively, conditions that imply a free Zn^{2+} concentration of 13 μM and 83 μM of $ZnATP^{2-}$. Again, the free Zn^{2+} concentration is below the optimal value and besides the concentration of the co-substrate is not saturating. Finally, under the experimental conditions employed by Lee et al. (2000) at pH 6.0, the free Zn^{2+} concentration of 31 μM is in the inhibitory range, and the concentration of the co-substrate either $ZnATP^{2-}$ or PL are not saturating. These conditions would also explain the differences in the k_{cat} values obtain in different reports. These examples highlighted the importance of an accurate estimation of the actual concentration of the species involved in order to obtain reliable values for the kinetic parameters, and for determine the true regulators of the enzymatic activity of PLK. Since brain, besides muscle and bone narrow, is a tissue rich in zinc and considering that this metal appears to be critical for cognitive functions (Canzoniero et al. 1999), regulation of human brain PLK by free zinc could be an important regulation mechanism of biological functions.

Acknowledgments This work was supported by Grants from the Comisión Nacional de Investigación Científica y Tecnológica, FONDECYT 1070111 and 1110137. We thank Dr. Ricardo Cabrera for helpful discussions. Finally, we gratefully acknowledge Dra. Linda McBroom-Cerajewski (Structural Genomic Consortium), from who expression vector containing hPLK was obtained (p24a-LIC-hPLK plasmid).

References

Abercrombie D, Martin D (1980) Inhibition of pyridoxal kinase by the pyridoxal-γ-aminobutyrate imine. J Biol Chem 255:79–84

Amsler PE, Sigel H (1976) Comparison of the metal–ion-promoted dephosphorylation of the 5′-triphosphates of adenosine, inosine, guanosine and cytidine by Mn^{2+}, Ni^{2+} and Zn^{2+} in binary and ternary complexes. Eur J Biochem 63:569–581

Canzoniero L, Turetsky D, Choi D (1999) Measurement of intracellular free zinc concentrations accompanying zinc-induced neuronal death. J Neurosci 19:1–6

Cao P, Gong Y, Tang L, Leung Y-C, Jiang T (2006) Crystal structure of human pyridoxal kinase. J Struct Biol 154:327–332

Cornish-Bowden A (1995) Fundamentals of enzyme kinetics (revised edition). Portland Press Ltd, London

di Salvo ML, Hunt S, Schirch V (2004) Expression, purification, and kinetic constants for human and *Escherichia coli* pyridoxal kinases. Protein Expr Purif 36:300–306

di Salvo ML, Contestabile R, Safo MK (2011) Vitamin B_6 salvage enzymes: mechanism, structure and regulation. Biochim Biophys Acta 1814:1597–1608

Gandhi AK, Ghatge MS, Musayev FN, Sease A, Aboagye SO, di Salvo ML, Schirch V, Safo MK (2009) Kinetic and structural studies of the role of the active site residue Asp235 of human pyridoxal kinase. Biochem Biophys Res Commun 381:12–15

Gandhi AK, Desai JV, Ghatge MS, di Salvo ML, Di Biase S, Danso-Danquah R, Musayev FN, Contestabile R, Schirch V, Safo MK (2012) Crystal structures of human pyridoxal kinase in complex with the neurotoxins, ginkgotoxin and theophylline: insights into pyridoxal kinase inhibition. PLoS ONE 7(7):e40954

Ismail S, Dimov S, Atanassova A, Tempel W, Arrowsmith C, Edwards A, Sundstrom M, Weigelt J, Bochkarev A, Park H (2005) Crystal structure of a human pyridoxal kinase. Structural Genomics Consortium. http://www.thesgc.org/structures/details?pdbid=2AJP

Jones DC, Alphey MS, Wyllie S, Fairlamb AH (2012) Chemical, genetic and structural assessment of pyridoxal kinase as a drug target in the African trypanosome. Mol Microbiol 86:1365–2958

Kästner U, Hallmen C, Wiese M, Leistner E, Drewke C (2007) The human pyridoxal kinase, a plausible target for ginkgotoxin from *Ginkgo biloba*. FEBS J 274:1036–1045

Lee H, Moon BJ, Choi SY, Kwon O (2000) Human pyridoxal kinase: overexpression and properties of the recombinant enzyme. Mol Cells 10:452–459

Li MH, Kwok F, Chang WR, Lau CK, Zhang JP, Lo SCL, Jiang T, Liang DC (2002) Crystal structure of brain pyridoxal kinase, a novel member of the ribokinase superfamily. J Biol Chem 277:46385–46390

Lum H, Kwok F, Lo S (2002) Cloning and characterization of *Arabidopsis thaliana* pyridoxal kinase. Planta 215:870–879

McCormick DB, Gregory ME, Snell EE (1961) Pyridoxal phosphokinases. I. Assay, distribution, purification and properties. J Biol Chem 236:2076–2084

Neary J, Diven W (1970) Purification, properties, and a possible mechanism for pyridoxal kinase from bovine brain. J Biol Chem 245:5585–5593

Newman JA, Das SK, Sedelnikova SE, Rice DE (2006) The crystal structure of an ADP complex of *Bacillus subtilis* pyridoxal kinase provides evidence for the parallel emergence of enzyme activity during evolution. J Mol Biol 363:520–530

Percudani R, Peracchi A (2003) A genomic overview of pyridoxal-phosphate-dependent enzymes. EMBO Rep 4: 850–854

Safo MK, Musayev FN, di Salvo ML, Hunt S, Claude JB, Schirch V (2006) Crystal structure of pyridoxal kinase from the *Escherichia coli* pdxK gene: implications for the classification of pyridoxal kinases. J Bacteriol 188:4542–4552

Sigel H (2004) Adenosine 5′-triphosphate (ATP^{4-}): aspects of the coordination chemistry of a multitalented biological substrate. Pure Appl Chem 76:375–388

Storer A, Cornish-Bowden A (1976) Concentration of $MgATP^{2-}$ and other ions in solution. Biochem J 159:1–5

Tribolet R, Sigel H (1988) Influence of protonation degree on the self-association properties of adenosine 5′-triphosphate (ATP). Eur J Biochem 170:617–626

Zhang Y, Dougherty M, Downs DM, Ealick SE (2004) Crystal structure of an aminoimidazole riboside kinase from *Salmonella enterica*: implications for the evolution of the ribokinase superfamily. Structure 12:1809–1821